Inorganic Chemistry

Article

pubs.acs.org/IC

Investigation of Mn, Fe, and Ni Incorporation in $CeCo_2Al_8$

LaRico J. Treadwell,[†,‡] Pilanda Watkins-Curry,[†,‡] Jacob D. McAlpin,[†] Drew J. Rebar,[§] Jessica K. Hebert,[§] John F. DiTusa,[§] and Julia Y. Chan*[,‡]

[†]Department of Chemistry and [§]Department of Physics and Astronomy, Louisiana State University, Baton Rouge, Louisiana 70803, United States

[‡]Department of Chemistry, University of Texas at Dallas, Richardson, Texas 75080, United States

Supporting Information

ABSTRACT: Single crystals of $CeCo_{2-x}M_xAl_8$ (M = Mn, Fe, Ni; $0 \le x < 1$) were grown and characterized by X-ray diffraction and magnetic susceptibility. The unit cell volumes of Mn-doped compounds increase and those of Ni-doped compounds decrease with increasing dopant concentration. All samples display a magnetic ordering near 6 K with magnetic moments of the analogues ranging from 2.61 to 2.81 μ_B/mol Ce and slightly higher than Ce^{3+} only magnetic moment. The unit cell volumes of Fe-doped compounds also increase with increasing Fe concentration. However, the cell volume of $CeCo_{2-x}Fe_xAl_8$ decreases for $x = 1.00$ and is not Curie–Weiss possibly because of valence fluctuation.

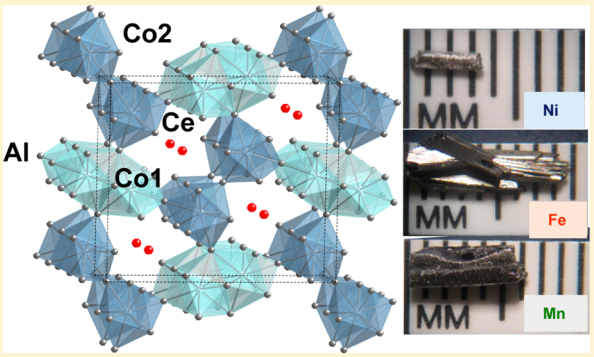

INTRODUCTION

The growth of single-crystalline Ce-intermetallic compounds has attracted our interest because of their unusual ground-state properties such as heavy Fermion behavior, non-Fermi liquid behavior, and valence fluctuations.[1,2] The magnetic ground state of Ce compounds can be determined by the relative strength of Ruderman–Kittel–Kasuya–Yosida (RKKY)[3] and Kondo interactions.[4,5] The magnetic moment associated with rare-earth atoms can be characterized by the magnetic moment that can be obtained from measurements of the magnetic susceptibility. A reduction in the magnetic moment can be due to crystal-electric-field or valence-fluctuating behavior. In Ce intermetallics that exhibit valence fluctuation, the rare-earth ions' valence can fluctuate between states having a magnetic moment and no appreciable magnetic moment. For example, $CeNiSi_2$ is a nonmagnetic intermediate valence material with a Kondo temperature $T_K \sim 500$ K. The unit cell volume of $Ce_2Co_3Ge_5$, for example, deviates from that of isostructural compounds and has a magnetic moment of ~0.95 μ_B with $\theta = -3.05$ K, indicating the valence-fluctuating nature of Ce.[6] CeRuSn is a mixed-valent compound with Ce^{3+} and Ce^{4+} cations, as evident by the bond distances. The shortened Ce–Ru bond distances cause stronger 4f-ligand hybridization, thereby leading to a 4+ Ce state.[7] Because of the unstable magnetic ground state of Ce intermetallics, substitution studies have also been investigated. For example, the Kondo lattice compound $CeNiGe_2$ orders antiferromagnetically at 3.3 K,[8] and upon substitution of Co for Ni, the antiferromagnetic ordering is suppressed and an intermediate valence is evident for $x > 0.5$.[9] There is also evidence of mixed-valent behavior in the $CeNi_{1-x}Cu_xAl$ ($0 < x < 0.3$) series because of the presence of small magnetic moments and non-Curie–Weiss behavior. This work illustrates transitions from the mixed-valent behavior of CeNiAl to the trivalent state in CeCuAl.[10] CeRuAl of the LaNiAl structure type exhibits intermediate valence behavior with no magnetic ordering,[11] while CeNiAl of the ZrNiAl structure type exhibits temperature-independent susceptibility, indicating that Ce ions are in a tetravalent state. The solid solution $CeRu_{1-x}Ni_xAl$ with $0.1 < x < 0.95$ has been investigated, and for $x < 0.85$, the compounds adopt the LaNiAl structure type and exhibit valence fluctuation, while for $x = 0.9–1$, the compounds adopt the ZrNiAl structure type.[12]

Our effort to study materials with competing magnetic interactions and unstable magnetic ground states has led us to grow and characterize Ce-containing compounds and to investigate substitution effects. In particular, compounds such as $CeCo_2Al_8$,[13] an intermetallic phase adopting the $CaCo_2Al_8$ structure type,[14] follows Curie–Weiss behavior with an effective moment consistent with Ce^{3+} with $\theta = -136(1)$ K, while neither Ce nor Fe carries a magnetic moment in $CeFe_2Al_8$.[13,15] We set out to grow single crystals of $CeCo_{2-x}M_xAl_8$ (M = Mn, Fe, Ni; $0 \le x < 1$) to investigate the effects of substitution on the structure and magnetic properties. Herein, we report the synthesis and crystal structures of $CeCo_{2-x}M_xAl_8$ (M = Mn, Fe, Ni; $0 \le x < 1$) and the properties of the Mn and Fe analogues.

Special Issue: To Honor the Memory of Prof. John D. Corbett

Received: September 27, 2014
Published: November 13, 2014

Table 1. Composition of $CeCo_{2-x}M_xAl_8$ (M = Mn, Fe, Ni)

	Mn			Fe			Ni		
nominal (x)	0.33	0.67	1.00	0.33	0.67	1.00	0.33	0.67	1.00
XRD (x)	0.22(5)	0.45(3)	0.70(4)	0.23(6)	0.67(8)	1.00(5)	0.29(5)	0.60(8)	0.71(7)
EDS (x)	0.29(3)	0.43(1)	0.71(2)	0.30(1)	0.61(3)	1.06(10)	0.24(2)	0.62(2)	0.80(4)

Table 2. Crystallographic Parameters of $CeCo_{2-x}M_xAl_8$ (M = Mn, Fe, Ni; $x < 0.33$)

compound	$CeCo_2Al_8$	$CeCo_{1.78(5)}Mn_{0.22(5)}Al_8$	$CeCo_{1.77(7)}Fe_{0.23(7)}Al_8$	$CeCo_{1.71(1)}Ni_{0.27(1)}Al_8$
cryst syst	orthorhombic	orthorhombic	orthorhombic	orthorhombic
space group	*Pbam*	*Pbam*	*Pbam*	*Pbam*
a (Å)	12.4720(2)	12.4844(10)	12.4770(5)	12.4770(10)
b (Å)	14.3870(3)	14.392(4)	14.391(2)	14.393(4)
c (Å)	4.0220(5)	4.026(3)	4.027(2)	4.023(4)
V (Å^3)	721.69(9)	723.5(6)	723.1(4)	722.5(7)
Z	4	4	4	4
cryst dimens (mm^3)	0.03 × 0.03 × 0.04	0.02 × 0.02 × 0.03	0.02 × 0.03 × 0.05	0.05 × 0.07 × 0.18
temperature (K)	293(2)	293(2)	293(2)	293(2)
θ range (deg)	2.83−31.01	2.20−31.00	3.27−31.00	3.27−31.19
μ (mm^{-1})	11.613	11.037	11.303	11.91
measd reflns	2191	2197	2194	2148
indep reflns	1297	1298	1300	1315
reflns with $I > 2\sigma(I)$	1141	970	1033	942
R_{int}	0.0243	0.0433	0.0284	0.0488
h	−17 to +17	−17 to +18	−17 to +18	−17 to +18
k	−20 to +20	−20 to +20	−20 to +20	−20 to +20
l	−5 to +5	−5 to +5	−5 to +5	−5 to +5
reflns/param	1297/70	1297/72	1300/71	1302/72
$\Delta\rho_{max}$ (e/Å^3)	1.119	1.541	2.459	1.441
$\Delta\rho_{min}$ (e/Å^3)	−2.148	−1.249	−1.272	−1.559
extinction coeff	0.0045(3)	0.0033(3)	0.0076(3)	0.0023(2)
GOF	1.179	1.046	1.039	1.032
R1(F)[a]	0.0256	0.0349	0.0266	0.0367
wR2[b]	0.0564	0.0756	0.0583	0.0702

[a] $R1 = \sum||F_o| - |F_c||/\sum|F_o|$. [b] $wR2 = [\sum[w(F_o^2 - F_c^2)^2]/\sum[w(F_o^2)^2]]^{1/2}$.

EXPERIMENTAL SECTION

Synthesis. The flux-growth method was selected to grow single crystals of $CeCo_{2-x}M_xAl_8$ (M = Mn, Fe, Ni; $0 \le x < 1$). This technique uses a low-melting metal as the solvent (flux), which enables metals with higher melting points to dissolve at relatively low temperature.[16,17] Ce (rod, 99.9%), Co (powder, 99.9%), M (Mn, Fe, and Ni powder, 99.9%), and Al (shots, 99.9%) were used as received. For $CeCo_2Al_8$, the elements Ce:Co:Al in atomic ratio 1:2:20, respectively, were placed in an alumina crucible, topped with another crucible, and sealed in an evacuated (50−70 mTorr) fused-silica tube filled with ~0.3 atm of Ar. The reaction was heated to 1200 °C at a rate of 100 °C/h and dwelled for 24 h. The ampule was subsequently cooled to 900 °C at a rate of 4 °C/h, followed by centrifugation to separate crystals from the Al flux. Single crystals of $CeCo_2Al_8$ were etched in dilute NaOH (~0.1 M) and then cleaned with dilute HNO_3 (~0.1 M). To synthesize $CeCo_{2-x}M_xAl_8$ (M = Mn, Fe, Ni; $0 \le x < 1$), the initial reaction ratios provided in Table 1 were used along with the aforementioned heating profile. Single crystals of $CeCo_{2-x}M_xAl_8$ (M = Mn, Fe, Ni; $0 \le x < 1$) were etched in dilute NaOH (~0.1 M) and then cleaned with dilute HNO_3 (~0.1 M).

Elemental Analysis. Elemental analysis was conducted via energy-dispersive spectroscopy (EDS) using a FEI Quanta 200 scanning electron microscope equipped with an energy-dispersive X-ray analysis (EDAX) detector at an accelerating voltage of 20 kV and a LEO 1530 VP scanning electron microscope equipped with an EDAX detector at an accelerating voltage of 19 kV. Spectra were integrated for 30 s, and the results from five spots were averaged and normalized to Ln to determine the atomic percentage of each element. The compositions are $Ce_{1.00(6)}Co_{1.47(5)}Mn_{0.29(3)}Al_{7.58(13)}$, $Ce_{1.00(10)}Co_{1.50(5)}Mn_{0.43(1)}Al_{7.97(19)}$, $Ce_{1.00(10)}Co_{1.28(3)}Mn_{0.71(2)}Al_{7.97(19)}$, $Ce_{1.00(3)}Co_{1.48(6)}Fe_{0.29(1)}Al_{9.43(9)}$, $Ce_{1.00(7)}Co_{1.30(6)}Fe_{0.55(3)}Al_{8.42(15)}$, $Ce_{1.00(5)}Co_{1.14(11)}Fe_{1.06(10)}Al_{7.58(25)}$, $Ce_{1.00(3)}Co_{1.73(2)}Ni_{0.24(3)}Al_{9.52(5)}$, $Ce_{1.00(3)}Co_{1.31(15)}Ni_{0.62(9)}Al_{8.48(18)}$, and $Ce_{1.00(3)}Co_{1.20(7)}Ni_{0.80(5)}Al_{8.48(18)}$.

Single-Crystal X-ray Diffraction (XRD). Fragments of $CeCo_{2-x}M_xAl_8$ (M = Mn, Fe, Ni; $0 \le x < 1$) single crystals were cut to suitable sizes and glued onto glass fibers with epoxy. The fibers were mounted on a Nonius Kappa CCD X-ray diffractometer equipped with a Mo Kα radiation source at room temperature. Also, fragments of $CeCo_{2-x}M_xAl_8$ (M = Mn, Fe, Ni; $0 \le x < 1$) single crystals were mounted on a Bruker D8 Quest Kappa single-crystal X-ray diffractometer equipped with a IμS microfocus source operating at 50 kV and 1 mA, a HELIOS optics monochromator, and a CMOS detector for multiple unit cell determinations. A starting model of the crystal structures was first obtained using *SIR92*[18] and refined with *SHELXL97*.[19] The atomic positions, site symmetries, displacement parameters, site occupancies, and interatomic distances of $CeCo_{2-x}M_xAl_8$ (M = Mn, Fe, Ni; $x < 0.33$) are provided in Tables 2−4. The crystallographic data for $CeCo_{2-x}M_xAl_8$ (M = Mn, Fe, Ni; $0.33 < x < 1$) are provided in the Supporting Information (SI). In the refinement of $CeCo_{2-x}M_xAl_8$ (M = Mn, Fe, Ni; $0 \le x < 1$), the dopant (M) was only modeled on the Co1 and Co2 sites, except for $CeCo_{2-x}Fe_xAl_8$ ($x = 0.33$), where Fe was only modeled on the Co1 site. Initially, structural models of $CeCo_{2-x}M_xAl_8$ (M = Mn, Fe, Ni; $0 \le x < 1$) were refined with the atomic positions of $CeCo_2Al_8$. The atomic displacement parameter (ADP) of the Co1 site was anomalously larger than Co2 ADP. Therefore, the dopant (M) was modeled first on the Co1 site and subsequently on the Co2 site. The dopant M in all refined models favored the Co1 position over the Co2

dx.doi.org/10.1021/ic502356t | *Inorg. Chem.* 2015, 54, 963−968

Table 3. Atomic Positions of $CeCo_{2-x}M_xAl_8$ (M = Mn, Fe, Ni; $x < 0.33$)

site	symmetry	x	y	z	occupancy	U_{eq} (Å^2)[a]
			$CeCo_2Al_8$			
Ce1	m	0.34038(2)	0.31841(2)	0	1	0.00837(11)
Co1	m	0.03488(6)	0.40566(5)	0	1	0.00693(16)
Co2	m	0.15166(5)	0.09643(5)	0	1	0.00565(15)
Al1	m	0.02559(13)	0.13168(11)	$^1/_2$	1	0.0075(3)
Al2	m	0.15953(12)	0.37939(11)	$^1/_2$	1	0.0075(3)
Al3	m	0.23625(13)	0.17238(10)	$^1/_2$	1	0.0077(3)
Al4	m	0.33139(13)	0.49140(11)	$^1/_2$	1	0.0080(3)
Al5	m	0.45285(13)	0.17938(10)	$^1/_2$	1	0.0070(3)
Al6	m	0.09584(12)	0.25276(10)	$^1/_2$	1	0.0078(3)
Al7	m	0.33993(12)	0.04446(11)	$^1/_2$	1	0.0097(3)
Al8	$2/m$	0	1/2	$^1/_2$	1	0.0076(4)
Al9	$2/m$	0	0	0	1	0.0082(4)
			$CeCo_{1.78(5)}Mn_{0.22(5)}Al_8$			
Ce1	m	0.34062(3)	0.31845(3)	0	1	0.01166(14)
Co1	m	0.03471(8)	0.40582(6)	0	0.81(5)	0.0094(10)
Mn1	m	0.03471(8)	0.40582(6)	0	0.19(5)	0.0094(10)
Co2	m	0.15142(8)	0.09656(6)	0	0.97(5)	0.0091(10)
Mn2	m	0.15142(8)	0.09656(6)	0	0.03(5)	0.0091(10)
Al1	m	0.02528(19)	0.13175(15)	0	1	0.0108(4)
Al2	m	0.15952(18)	0.37937(15)	0	1	0.0108(4)
Al3	m	0.23608(12)	0.17253(15)	$^1/_2$	1	0.0113(4)
Al4	m	0.3310(12)	0.49133(14)	$^1/_2$	1	0.0108(4)
Al5	m	0.45225(18)	0.17956(14)	$^1/_2$	1	0.0101(4)
Al6	m	0.09588(18)	0.25306(15)	$^1/_2$	1	0.0110(4)
Al7	m	0.33939(19)	0.04448(15)	$^1/_2$	1	0.0118(4)
Al8	$2/m$	0	1/2	$^1/_2$	1	0.0107(6)
Al9	$2/m$	0	0	0	1	0.0125(6)
			$CeCo_{1.77(7)}Fe_{0.23(6)}Al_8$			
Ce1	m	0.34072(2)	0.318513(19)	0	1	0.01055(11)
Co1	m	0.03456(5)	0.40589(5)	0	0.77(6)	0.0092(2)
Fe1	m	0.03456(5)	0.40589(5)	0	0.23(6)	0.0092(2)
Co2	m	0.15116(5)	0.09671(4)	0	1	0.00808(15)
Al1	m	0.02558(12)	0.13172(10)	$^1/_2$	1	0.0097(3)
Al2	m	0.15961(12)	0.37917(11)	$^1/_2$	1	0.0095(3)
Al3	m	0.23606(12)	0.17258(10)	$^1/_2$	1	0.0096(3)
Al4	m	0.33146(12)	0.49159(10)	$^1/_2$	1	0.0106(3)
Al5	m	0.45250(12)	0.17965(10)	$^1/_2$	1	0.0095(3)
Al6	m	0.09581(12)	0.25304(9)	0	1	0.0096(3)
Al7	m	0.33940(12)	0.04452(10)	0	1	0.0111(3)
Al8	$2/m$	0	1/2	$^1/_2$	1	0.0096(4)
Al9	$2/m$	0	0	0	1	0.0104(4)
			$CeCo_{1.71(1)}Ni_{0.27(1)}Al_8$			
Ce1	m	0.34045(4)	0.31846(3)	0	1	0.01140(14)
Co1	m	0.03474(8)	0.40566(7)	0	0.71(1)	0.0096(3)
Ni1	m	0.03474(8)	0.40566(7)	0	0.27(1)	0.0096(3)
Co2	m	0.15175(8)	0.09647(7)	0	1	0.0084(2)
Al1	m	0.02525(19)	0.13187(15)	$^1/_2$	1	0.0101(5)
Al2	m	0.1597(2)	0.37941(16)	$^1/_2$	1	0.0104(4)
Al3	m	0.23657(2)	0.17249(16)	$^1/_2$	1	0.0107(5)
Al4	m	0.3318(2)	0.49153(15)	$^1/_2$	1	0.0103(5)
Al5	m	0.45226(18)	0.17961(16)	$^1/_2$	1	0.0108(5)
Al6	m	0.0961(2)	0.25283(16)	0	1	0.0108(4)
Al7	m	0.3399(2)	0.04440(16)	0	1	0.0116(5)
Al8	$2/m$	0	1/2	$^1/_2$	1	0.0101(7)
Al9	$2/m$	0	0	0	1	0.0111(7)

[a] U_{eq} is defined as one-third of the trace of the orthogonalized U_{ij} tensor.

dx.doi.org/10.1021/ic502356t | Inorg. Chem. 2015, 54, 963−968

Table 4. Selected Interatomic Distances (Å) of $CeCo_{2-x}M_xAl_8$ (M = Mn, Fe, Ni; $x < 0.33$)

		$CeCo_2Al_8$	$CeCo_{1.78(5)}Mn_{0.22(5)}Al_8$	$CeCo_{1.77(7)}Fe_{0.23(7)}Al_8$	$CeCo_{1.71(1)}Ni_{0.27(1)}Al_8$
Ce	Al1 × 2	3.1457(16)	3.1493(11)	3.1443(14)	3.142(2)
	Al2 × 2	3.1467(14)	3.1541(11)	3.1500(13)	3.147(2)
	Al3 × 2	3.1851(15)	3.1941(11)	3.1891(13)	3.184(2)
	Al4 × 2	3.2017(16)	3.2118(11)	3.2049(14)	3.203(2)
	Al5 × 2	3.1643(15)	3.1620(11)	3.1611(13)	3.160(2)
M1	Al2 × 2	2.5698(14)	2.5863(10)	2.5761(13)	2.573(2)
	Al5 × 2	2.5667(14)	2.5856(10)	2.5726(12)	2.571(2)
	Al6 × 1	2.3275(16)	2.3437(15)	2.3287(15)	2.329(3)
	Al7 × 2	2.5349(17)	2.5476(16)	2.5375((16)	2.535(3)
	Al8 × 2	2.4649(17)	2.4591(4)	2.4646(9)	2.4653(17)
	M1 × 1	2.8505(13)	2.8135(13)	2.8426(13)	2.851(2)
M2	Al1 × 2	2.6026(15)	2.6024(10)	2.6005(13)	2.607(2)
	Al3 × 2	2.5201(14)	2.5259(10)	2.5236(13)	2.523(2)
	Al4 × 2	2.5243(14)	2.5334(10)	2.5278(13)	2.524(2)
	Al6 × 1	2.3543(16)	2.3558(15)	2.3532(15)	2.355(3)
	Al7 × 1	2.4643(17)	2.4592(16)	2.4658(16)	2.464(3)
	Al9 × 1	2.3457(7)	2.3462(6)	2.3439(6)	2.3480(11)

site, which is different from the previously reported $YbNi_{2-x}Fe_xAl_8$ (x = 0.91), where the dopant (Fe) preferred the Ni2 site.[20] The concentrations of M from the structural refinement of $CeCo_{2-x}M_xAl_8$ (M = Fe, Ni; $0 \le x < 1$) are provided in Table 1.

Physical Properties. The direct-current (DC) magnetization was measured in a Quantum Design Superconducting Quantum Interference Device (SQUID) magnetometer with the temperature-dependent susceptibility measured between 1.8 and 400 K with an applied magnetic field of 0.1 T. The field dependence of the magnetization data was measured at 2 and 300 K with fields of up to 7 T. Alternating-current (ac) susceptibility measurements were carried out at a frequency of 13 kHz and an amplitude of 1 Oe between 2 and 20 K to confirm the magnetic ordering observed in the dc susceptibility.

RESULTS AND DISCUSSION

Crystal Structure. $CeCo_{2-x}M_xAl_8$ (M = Mn, Fe, Ni; $0 \le x < 1$) adopts the $CaCo_2Al_8$ structure type[14] with the orthorhombic space group *Pbam*. This structure type has also been reported for $LnRu_2Ga_8$ (Ln = Ce, Pr),[21] $PrCo_2Al_8$,[22] and $YbNi_{2-x}Fe_xAl_8$ (x = 0.91).[20] There are 12 unique crystallographic positions in $CeCo_2Al_8$ consisting of one Ce, two Co, and nine Al atoms. The crystal structure of $CeCo_2Al_8$ is shown in Figure 1 and consists of Ce atoms encapsulated in channels created by the Co sublattice. Each Ce atom is located in a pentagonal prism of Al atoms with distances of ~3.1 Å. All of the faces of the pentagonal prisms are capped by Al atoms with Ce−Al distances ranging from 3.3 to 4.0 Å. The transition-metal sublattice of $CeCo_2Al_8$ can be described as open channels formed by corner-sharing Co1 and Co2 polyhedra, with Ce atoms residing in the center. The Co1 and Co2 environments are nine-coordinate, consisting of Al atoms forming mono-capped rectangular prisms. The Co1 monocapped rectangular prisms are face-sharing with Co1 polyhedra, forming dimers with a Co1−Co1 distance of 2.8506(3) Å. The Co−Al distances in the $[CoAl_{8+1}]$ prisms range from ~2.3 to 2.5 Å, which is comparable to the sum of the radii of Co (1.26) and Al (1.18),[23] suggesting strong atomic interactions. The Co−Al interatomic distances are also comparable to the bond interaction in Co_2Al_9,[24,25] with Co−Al distances ranging from 2.3 to 2.5 Å. The shortest Ce−Al distances and the Co−Al distances in $[CoAl_{8+1}]$ prisms are comparable to the sum of the radii (3.25 Å for Ce + Al and 2.47 Å for Co + Al), suggesting that strong interactions are present in $CeCo_2Al_8$.

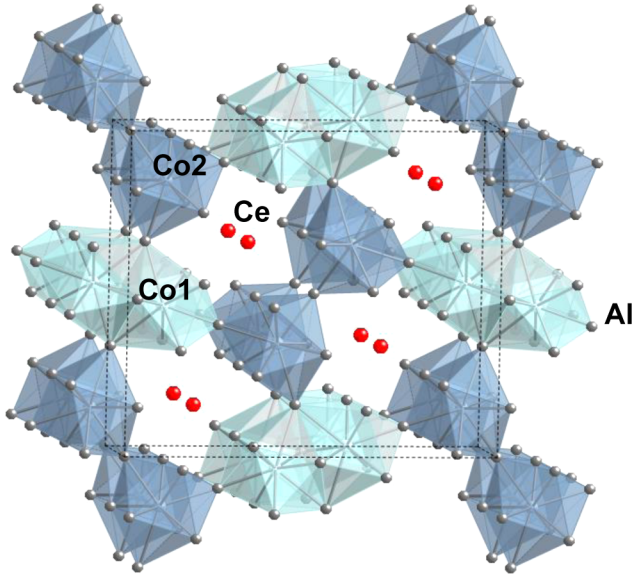

Figure 1. Crystal structure of $CeCo_2Al_8$ in the c direction. Co1 and Co2 are represented as light-blue and dark-blue polyhedra, respectively.

A plot of the volume as a function of the dopant in $CeCo_{2-x}M_xAl_8$ (M = Mn, Fe, Ni; $0 \le x < 1$) is shown in Figure 2. For Mn-doped compounds, there is a steady increase in the volume, which is consistent with Mn substituting for Co, causing an expansion of the crystal lattice. For Fe-doped compounds, the volumes increase as a function of the concentration until x = 1.00(5), where the volume decreases significantly. This behavior can be attributed to valence fluctuation of Ce atoms between Ce^{3+} ($4f^1$) and Ce^{4+} ($4f^0$). Valence fluctuation is also observed with the end member $CeFe_2Al_8$.[26] In Ni-doped $CeCo_2Al_8$, a slight increase in the volume is observed for x = 0.29(5), which is followed by a decrease in the volume as the Ni concentration increases, consistent with the presence of a smaller atom.

Magnetism. The field-dependent magnetization of $CeCo_{2-x}M_xAl_8$ (M = Mn, Fe; $0 \le x < 1$) at 2 K in applied fields up

dx.doi.org/10.1021/ic502356t | Inorg. Chem. 2015, 54, 963−968

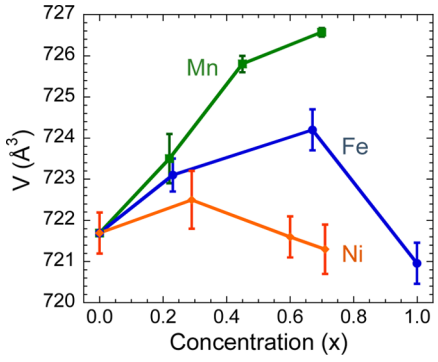

Figure 2. Volume of $CeCo_{2-x}M_xAl_8$ (M = Mn, Fe, Ni; $0 < x < 1$).

to 7 T is shown in Figures 3 and 4. The low-field magnetization displays a hysteresis consistent with a small ferromagnetically

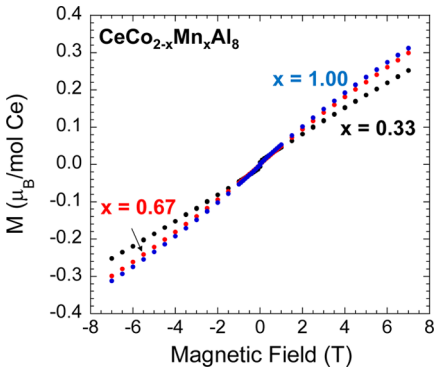

Figure 3. Field-dependent magnetization of $CeCo_{2-x}Mn_xAl_8$ ($0 < x < 1.00$).

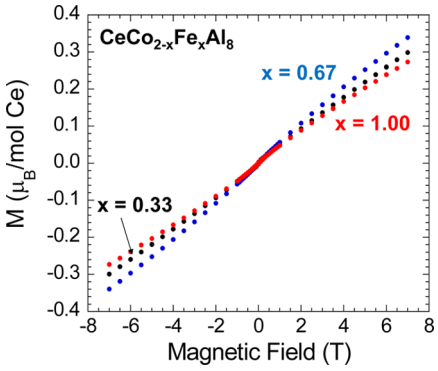

Figure 4. Field-dependent magnetization of $CeCo_{2-x}Fe_xAl_8$ ($0 < x < 1.00$).

ordered moment. At higher fields (>1 T), the magnetization is linear in fields up to 7 T. In contrast, the field-dependent magnetization of $CeCo_{2-x}M_xAl_8$ (M = Mn, Fe; $0 \leq x < 1$) at 300 K exhibits a linear field dependence with no hysteretic behavior, indicating that there is a magnetic phase transition between these two temperatures. The magnetic moment reaches a maximum of ~0.35 μ_B/mol Ce at 7 T for all compounds. This value is significantly less than the calculated μ_{sat} for a Ce^{3+} ion (2.14 μ_B/mol Ce) because the magnetization shows no sign of saturation in our field range. However, it is similar to the previously reported magnetic data on the polycrystalline sample of $CeCo_2Al_8$.[13] The high-field magnetization shows a small systematic increase with Mn doping, consistent with a small magnetic moment likely associated with the transition-metal site in addition to the Ce^{3+} moment found in $CeCo_2Al_8$. In contrast, Fe substitution yields an increasing magnetic moment only up to $x = 0.67$. For $x = 1.0$, we find a decreased magnetic moment suggestive of the valence fluctuations seen in $CeFe_2Al_8$, consistent with our cell volume.

Figures 5 and 6 show the temperature-dependent susceptibility of $CeCo_{2-x}M_xAl_8$ (M = Mn, Fe; $0 \leq x < 1$) measured

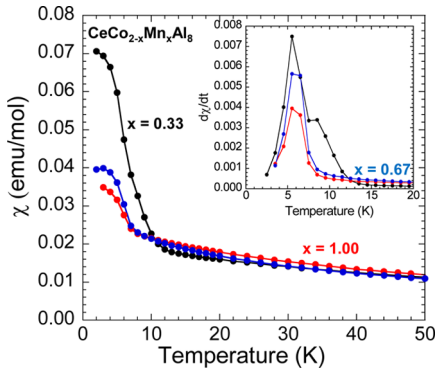

Figure 5. Temperature-dependent magnetization of $CeCo_{2-x}Mn_xAl_8$ ($0 < x < 1.00$). The inset shows $d\chi/dt$ of $CeCo_{2-x}Mn_xAl_8$ ($0 < x < 1.00$).

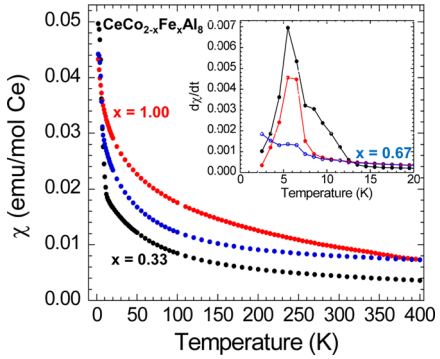

Figure 6. Temperature-dependent magnetization of $CeCo_{2-x}Fe_xAl_8$ ($0 < x < 1.00$). The inset shows $d\chi/dt$ of $CeCo_{2-x}Fe_xAl_8$ ($0 < x < 1.00$).

with an applied field of 0.1 T. The susceptibility of all compounds displays a Curie–Weiss behavior at temperatures above 70 K, with the exception of $CeCo_{2-x}Fe_xAl_8$ ($x = 1.00$), which cannot be fit satisfactorily with this form. At temperatures below 10 K, all are magnetically ordered and can be determined from the maximum in $d\chi/dt$, as shown in the insets of Figures 5 and 6. The transition temperatures are confirmed with ac susceptibility, as provided in the SI. It is clear from the magnetic data that the transition temperature in $CeCo_{2-x}M_xAl_8$ (M = Mn, Fe; $0 \leq x < 1$) does not vary as a function of the chemical substitution concentration. The magnetic susceptibility of $CeCo_{2-x}M_xAl_8$ (M = Mn, Fe; $0 \leq x < 1$) can be fit with a Curie–Weiss relationship, with the exception of $x = 1.00$ for Fe substitution. The effective moments of $CeCo_{2-x}Mn_xAl_8$ ($0 \leq x < 1$) are 2.71(4), 2.73(5), and 2.81(3) μ_B with Weiss constants of −38.5(3), −37.7(3), and −30.27(5) K for $x \sim$ 0.33, 0.67, and 1.00, respectively. The magnetic susceptibility of $CeCo_{2-x}Fe_xAl_8$ ($0 < x < 0.67$) was fit to a Curie–Weiss equation and yielded μ_{eff} values of 2.73(9) and 2.61(7) μ_B and Weiss constants of −48.1(7) and −23.5(6) K, respectively. The Weiss constants are decreasing, indicating that the strength of

dx.doi.org/10.1021/ic502356t | Inorg. Chem. 2015, 54, 963–968

antiferromagnetic exchange interactions is decreasing with x. The magnetic susceptibility of $CeCo_{2-x}Fe_xAl_8$ (x = 1.00) cannot be fit to the Curie−Weiss relationship and hence is likely due to valence fluctuation, consistent with the change in the volume for x = 1.00. Detailed physical property measurements of the Ni analogues are under investigation.

CONCLUSION

We have synthesized and investigated the structures of $CeCo_{2-x}M_xAl_8$ (M = Mn, Fe, Ni; $0 \leq x < 1$). By substituting and controlling the amount of the dopant (M) in $CeCo_{2-x}M_xAl_8$ (M = Mn, Fe, Ni; $0 \leq x < 1$), we can systematically investigate the effects of substitution on the structural and physical properties of $CeCo_2Al_8$. The expansion and contraction of the volume of $CeCo_{2-x}M_xAl_8$ (M = Mn, Fe, Ni; $0 \leq x < 1$) follow the expected trend given by the dopant (M) identity, except for $CeCo_{2-x}Fe_xAl_8$ [x = 1.00(5)], which represents the concentration determined to exhibit valence fluctuation. It appears from our structural data that the 4f electronic state of Ce is not affected by the size of the dopant atom. $CeCo_{2-x}M_xAl_8$ (M = Mn, Fe; $0 \leq x < 1$) displays hysteretic behavior in the field-dependent magnetization, indicating a small ferromagnetic moment at low fields. At higher fields, the magnetization increases linearly to 7 T. The effective moments determined from fitting the Curie−Weiss relation $\chi(T)$ of $CeCo_{2-x}M_xAl_8$ (M = Mn, Fe; $0 \leq x < 1$) are higher than the magnetic moment for a free Ce^{3+} ion (2.54 μ_B). These magnetic moments, however, display a small systematic variation with substitution consistent with the changes that we observe in $M(H)$. However, we were unable to obtain an effective moment for $CeCo_{2-x}Fe_xAl_8$ ($x \sim 1$) because of the unusual temperature dependence in the magnetic susceptibility that is likely due to valence fluctuations.

ASSOCIATED CONTENT

Supporting Information

Additional temperature- and field-dependent data, additional crystallographic data summarized in tables detailing the crystallographic details of $CeCo_{2-x}M_xAl_8$ (M = Mn, Fe, Ni; $0 \leq x < 1$), and X-ray crystallographic data in CIF format for all compounds. This material is available free of charge via the Internet at http://pubs.acs.org.

AUTHOR INFORMATION

Corresponding Author

*E-mail: Julia.Chan@utdallas.edu. Tel: (972)883-3595.

Notes

The authors declare no competing financial interest.

ACKNOWLEDGMENTS

J.Y.C. acknowledges financial support from the National Science Foundation (NSF; Grant DMR1358975) and the Department of Energy, Office of Basic Energy Sciences (Grant DE-FG02-08ER4652). J.F.D. acknowledges support from the NSF (Grant DMR1206763).

REFERENCES

(1) Phelan, W. A.; Menard, M. C.; Kangas, M. J.; McCandless, G. T.; Drake, B. L.; Chan, J. Y. *Chem. Mater.* **2012**, *24*, 409−420.
(2) Edelstein, A. S. *J. Magn. Magn. Mater.* **2003**, *256*, 430−448.
(3) Ruderman, M. A.; Kittel, C. *Phys. Rev.* **1954**, *96*, 99−102.
(4) Kondo, J. *Prog. Theor. Phys.* **1964**, *32*, 37−48.
(5) Yang, Y.-f.; Fisk, Z.; Lee, H.-O.; Thompson, J. D.; Pines, D. *Nature* **2008**, *454*, 611−613.
(6) Layek, S.; Anand, V. K.; Hossain, Z. *J. Magn. Magn. Mater.* **2009**, *321*, 3447−3452.
(7) Fikáček, J.; Prokleška, J.; Prchal, J.; Custers, J.; Sechovský, V. *J. Phys.: Condens. Matter* **2013**, *25*, 1−6.
(8) Hong, S. O.; Mun, E. D.; Kwon, Y. S. *Physica B* **2003**, *329−333* (Part 2), 514−515.
(9) Moon, E. D.; Hong, S. O.; Kim, D. L.; Ri, H. C.; Kwon, Y. S. *Physica B* **2003**, *329−333* (Part 2), 516−517.
(10) Cermáka, P.; Javorskýa, P.; Šantaváb, E. *Acta Phys. Polym., A* **2010**, *118*, 926−928.
(11) Gribanov, A. V.; Tursina, A. I.; Grytsiv, A. V.; Murashova, E. V.; Bukhan'ko, N. G.; Rogl, P.; Seropegin, Y. D.; Giester, G. *J. Alloys Compd.* **2008**, *454*, 164−167.
(12) Niehaus, O.; Rodewald, U. C.; Abdala, P. M.; Touzani, R. S.; Fokwa, B. P. T.; Janka, O. *Inorg. Chem.* **2014**, *53*, 2471−2480.
(13) Ghosh, S.; Strydom, A. M. *Acta Phys. Polym., A* **2011**, *121*, 1082−1084.
(14) Czech, E.; Cordier, G.; Schäfer, H. *J. Less Common Met.* **1983**, *95*, 205−211.
(15) Tamura, I.; Mizushima, T.; Isikawa, Y.; Sakurai, J. *J. Magn. Magn. Mater.* **2000**, *220*, 31−38.
(16) Canfield, P. C.; Fisk, Z. *Philos. Mag.* **1992**, *65*, 1117−1123.
(17) Kanatzidis, M. G.; Pöttgen, R.; Jeitschko, W. *Angew. Chem., Int. Ed.* **2005**, *44*, 6996−7023.
(18) Altomare, A.; Burla, M. C.; Camalli, M.; Cascarano, G. L.; Giacovazzo, C.; Guagliardi, A.; Moliterni, A. G. G.; Polidori, G.; Spagna, R. *J. Appl. Crystallogr.* **1999**, *32*, 115−119.
(19) Sheldrick, G. *Acta Crystallogr.* **2008**, *64*, 112−122.
(20) Wu, X.; Francisco, M.; Rak, Z.; Bakas, T.; Mahanti, S. D.; Kanatzidis, M. G. *J. Solid State Chem.* **2008**, *181*, 3269−3277.
(21) Schlüter, M.; Jeitschko, W. *Inorg. Chem.* **2001**, *40*, 6362−6368.
(22) Tougait, O.; Kaczorowski, D.; Noël, H. *J. Solid State Chem.* **2005**, *178*, 3639−3647.
(23) Cordero, B.; Gomez, V.; Platero-Prats, A. E.; Reves, M.; Echeverria, J.; Cremades, E.; Barragan, F.; Alvarez, S. *Dalton Trans.* **2008**, 2832−2838.
(24) Antonyshyn, I.; Prots, Y.; Margiolaki, I.; Schmidt, M. P.; Zhak, O.; Oryshchyn, S.; Grin, Y. *J. Solid State Chem.* **2013**, *199*, 141−148.
(25) Pauling, L. *Acta Crystallogr.* **1951**, *4*, 138−140.
(26) Kolenda, M.; Koterlin, M. D.; Hofmann, M.; Penc, B.; Szytuła, A.; Zygmunt, A.; Żukrowski, J. *J. Alloys Compd.* **2001**, *327*, 21−26.